Special Issue Article

Journal of PeptideScience

Received: 30 October 2012 Revised: 22 November 2012 Accepted: 23 November 2012 Published online in Wiley Online Library: 27 December 2012

(wileyonlinelibrary.com) DOI 10.1002/psc.2475

Spectroscopically labeled peptaibiotic analogs: the 4-nitrophenylalanine infrared absorption probe inserted at different positions into trichogin GA IV‡

Cristina Peggion,[a]* Barbara Biondi,[a] Marta De Zotti,[a] Simona Oancea,[b] Fernando Formaggio[a] and Claudio Toniolo[a]

A set of three analogs of the 10-residue, membrane-active lipopeptaibiotic trichogin GA IV, labeled with the promising 4-nitrophenylalanine IR absorption probe for local polarity, was synthesized by the solid-phase methodology, chromatographically purified, and extensively characterized. A single residue modification was inserted near the N-terminus, in the central region, or at the C-terminus. A solution conformational analysis, carried out by FT-IR absorption, CD, and 2D-NMR combined with molecular dynamics calculations, indicates that the mono-labeled analogs maintain the overall helical properties of the parent compound. Membrane permeabilization measurements and antimicrobial tests revealed that they possess membrane-modifying properties and *in vitro* antibacterial activities analogous to those of the natural lipopeptaibiotic. Our IR absorption and attenuated total reflectance investigations in various environments, from which water was excluded for solubility reasons, showed that the 1350 cm^{-1} 4-nitrobenzyl band is a reporter group of rather limited sensitivity. Copyright © 2012 European Peptide Society and John Wiley & Sons, Ltd.

Keywords: antibacterial activitiy; conformation analysis; infrared absorption; membrane activity; 4-nitrophenylalanine; peptaibol synthesis

Introduction

Peptaibiotics are members of a unique class of membrane-active compounds of fungal origin [1]. These antibiotic peptides are characterized by a linear sequence of up to 19 α-amino acids, a very high percentage of the C^{α}-tetrasubstituted and strong helical inducer Aib (α-aminoisobutyric acid) residue [2–4], an N-terminal acyl group, and a C-terminal 1,2-(or β-)amino alcohol. The long-sequence peptaibiotics, e.g. alamethicin, generate channels in the membranes thereby modifying their permeability even in the absence of a voltage [5,6]. The short-sequence peptaibiotics, which possess a fatty acyl chain at the N-terminus, are referred to lipopeptaibiotics [7–9].

Trichogin GA IV, isolated by Auvin-Guette *et al.* [10] from *Trichoderma longibrachiatum*, is the most extensively investigated lipopeptaibiotic. Its amino acid sequence is given in the following, where *n*Oct is *n*-octanoyl and Lol is leucinol.

$$\overset{1}{n}\text{Oct-Aib-Gly-Leu-Aib-}\overset{5}{\text{Gly}}\text{-Gly-Leu-Aib-}\overset{10}{\text{Gly}}\text{-Ile-Lol}$$

In a series of collaborative efforts, we have recently shown that trichogin GA IV, and its easier-to-synthesize [Leu^{11}-OMe] (OMe, methoxy) analog as well, are slightly amphiphilic, right-handed, mixed 3_{10}-/α-helical [11–13] peptides with a remarkable capability to alter significantly the membrane permeability despite having a peptide main-chain too short to span it completely [14–16].

In recent years, we and others performed a systematic study of a large set of synthetic trichogin GA IV analogs and short sequences thereof by use of a variety of physico-chemical techniques with the aim at explaining in detail the mechanism of interactions of this lipopeptaibiotic with membrane model systems [15–40].

To further expand this ongoing project, in this work, we synthesized, characterized, and investigated the 3D structural, biological, and spectroscopic properties of three Phe(NO_2) (4-nitrophenylalanine)-containing analogs of trichogin GA IV, each labeled with a side-chain nitrobenzyl IR absorption probe [41,42]. These chromophoric residues were incorporated at position 3, 7, or 10, i.e. near the N-terminus, near the center, or near the C-terminus of the trichogin GA IV sequence, where they replace other hydrophobic residues, namely Leu, Leu, or Ile, respectively.

Phe(NO_2) is a remarkable residue due to its recently described properties: (i) It can be genetically, position-specifically, incorporated with high yield and fidelity into proteins [43–45] and synthetically into peptides. (ii) Its nitroaromatic moiety is able to quench the intrinsic fluorescence of nearby Trp residues or the artificially generated fluorescence of 1-pyrenyl-alanine

* *Correspondence to: Cristina Peggion, Department of Chemistry, University of Padova, via Marzolo 1, 35131 Padova, Italy. E-mail: cristina.peggion@unipd.it*

‡ *Special issue devoted to contributions presented at the 13th Naples Workshop on Bioactive Peptides, June 7–10, 2012, Naples.*

a *ICB, Padova Unit, CNR, Department of Chemistry, University of Padova, via Marzolo 1, 35131, Padova, Italy*

b *Department of Biochemistry and Toxicology, University 'Lucian Blaga', 550012, Sibiu, Romania*

or *para*-anthraniloyl-α,β-diaminopropionic acid inserted into proteins via site-directed mutagenesis [43–45]. (iii) It can serve as an efficient IR absorption reporter for vibrational energy arrival (heat transfer) to this amino acid from a distant, excited moiety in the peptide chain [42]. (iv) It represents a potentially useful IR absorption sensor of the environment polarity if inserted into a globular protein [41] or, by extrapolation, into a membrane-active peptide. In this article, we describe our results on the trichogin GA IV analogs mentioned earlier where we examined this last Phe(NO_2) property.

Materials and Methods

Solid-Phase Peptide Synthesis and Characterization of the Final Products

Fmoc-Phe(NO_2)-OH (Fmoc, fluorenyl-9-methoxycarbonyl) was a Bachem (Bubendorf, Switzerland) product. The other Fmoc-amino acids were supplied from Novabiochem (Merck Biosciences, La Jolla, CA). All other amino acid derivatives and reagents for peptide synthesis were purchased from Sigma-Aldrich (St. Louis, MO). Assembly of peptides on the Advanced ChemTech (Louisville, KY) 348 Ω peptide synthesizer was performed on a 0.044 mmol scale by the FastMoc methodology starting with the Lol-substituted 2-chlorotrityl resin (Iris Biotech, Marktredwitz, Germany) [46–48] (110 mg, loading 0.40 mmol/g). Each of the three syntheses required about 30 h. Most of the peptides bonds (those involving protein amino acids only) were formed by the use of *O*-(benzotriazol-1-yl)-1,1,3,3-tetramethyluronium hexafluorophosphate (HBTU) [49,50], 1-hydroxy-benzotriazole (HOBt) [51], *N*,*N*′-diisopropylethylamine, single acylation, 45 min coupling time, and N-methylpyrrolidin-2-one as the solvent. Five of the six coupling steps of the three Aib residues [52], performed in the presence of the strongly activating agent *O*-(7-azabenzotriazol-1-yl)-1,1,3,3-tetramethyluronium hexafluorophosphate (HATU) [49,50], were doubled and followed by a capping procedure using acetic anhydride in a large excess. Removal of the Fmoc N^{α}-protecting group was carried out with a 20% piperidine solution in *N*,*N*-dimethylformamide. The *n*Oct moiety at the N-terminus was introduced on the Aib residue at position 1 in the last synthetic step by exploiting the preformed activated ester of *n*-octanoic acid, obtained by reaction with an equivalent amount of *N*-ethyl-*N*′-[3-(dimethylamino) propyl] carbodiimide (EDC) and 7-aza-1-hydroxybenzotriazole (HOAt) [49,50] in the presence of *N*-methylmorpholine. The yields of the final purified products were 79–83% (40–43 mg, equivalent to 0.035–0.037 mmol, each). The purity percentage of the final crude materials was 90–92%. The peptides cleaved from the resin were filtered and collected. This step was repeated three times. The solutions were concentrated under a flow of nitrogen. The crude peptides were purified by reversed-phase chromatography on SepPak (Waters, Milford, MA) C_{18} column using eluants with different composition from pure water to 100% CH_3CN. The fractions collected were characterized by analytical RP-HPLC on a Jupiter Phenomenex (Torrance, CA) C_{18} column (4.6 × 250 mm, 5 μ, 300 Å) using an Agilent (Santa Clara, CA) 1200 HPLC pump. The binary elution system used was (A) 0.05% TFA (trifluoroacetic acid) in H_2O; (B) 0.05% TFA in CH_3CN/H_2O (9:1 v/v); gradient 60–90% B in 20 min (flow rate 1 ml/min); spectrophotometric detection at λ = 216 nm. Electrospray ionization mass spectrometry was performed by using a PerSeptive Biosystem Mariner instrument (Framingham, MA). The amino acid sequences, mass spectral data, and HPLC retention times of the final products are reported in Table 1. The HPLC elution profiles are shown in Figure 1. Complete ^{1}H NMR (400 MHz Bruker Advance DRX model) characterizations in 99.8% d_3 CD_3CN (Euriso-top, Saint Aubin, France) are given in the following text. Despite various attempts, none of the final peptides furnished any single crystal suitable for an X-ray diffraction analysis.

Trichogin GA IV [Phe(NO_2)]^3 analog

^{1}H NMR (400 MHz, CD_3CN): 8.138 (m, 2H, Phe(NO_2)^3 arom.); 7.926 (d, 1H, Phe(NO_2)^3 NH); 7.854 (t, 1H, Gly^6 NH); 7.736 (t, 1H, Gly^5 NH); 7.599 (s, 1H, Aib^4 NH); 7.596 (s, 1H, Aib^8 NH); 7.568 (t, 1H, Gly^9 NH); 7.509 (m, 2H, Phe(NO_2)^3 arom.); 7.496 (d, 1H, Leu^7 NH); 7.482 (t, 1H, Gly^2 NH); 7.335 (d, 1H, Ile^{10} NH); 7.258 (s, 1H, Aib^1 NH); 6.839 (d, 1H, Lol^{11} NH); 4.494 (m, 1H, Phe(NO_2)^3 α-CH); 4.096 (m, 1H, Leu^7 α-CH); 4.037 (m, 1H, Ile^{10} α-CH); 3.962 (m, 1H,

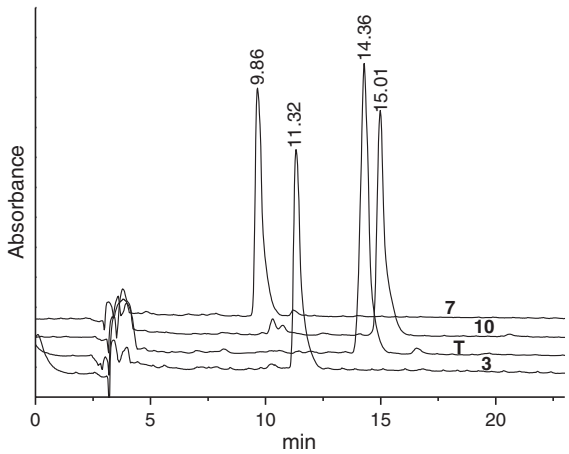

Figure 1. Analytical HPLC elution profiles (retention times) of (T) trichogin GA IV, (3) the [Phe(NO_2)]^3 analog, (7) the [Phe(NO_2)]^7 analog, and (10) the [Phe(NO_2)]^{10} analog. Experimental conditions: Jupiter Phenomenex C_{18} reversed phase column; gradient from 60% to 90% B in 20 min, where A = 0.05% TFA in a 9:1 (v/v) mixture of H_2O/CH_3CN and B = 0.05% TFA in a 1:9 (v/v) mixture of H_2O/CH_3CN. The absorption was monitored at 220 nm.

Table 1. Amino acid sequences, molecular masses, and retention times of the synthetic Phe(NO_2) trichogin GA IV analogs studied

Peptide	Amino acid sequence	$[M+H]^+_{calcd}$	$[M+H]^+_{exptl}$[a]	Retention time (min)
[Phe(NO_2)]^3-analog	*n*Oct-Aib-Gly-Phe(NO_2)-Aib-Gly-Gly-Leu-Aib-Gly-Ile-Lol	1145.70	1145.69	11.32
[Phe(NO_2)]^7-analog	*n*Oct-Aib-Gly-Leu-Aib-Gly-Gly- Phe(NO_2)-Aib-Gly-Ile-Lol	1145.70	1145.69	9.86
[Phe(NO_2)]^{10}-analog	*n*Oct-Aib-Gly-Leu-Aib-Gly-Gly-Leu-Aib-Gly- Phe(NO_2)-Lol	1145.70	1145.70	15.01

[a]Determined using ESI mass spectrometry (for details, see section on Materials and Methods).

Lol[11] α-CH); 3.8 (m, 2H, Gly[6] α-CH); 3.753(dd, 1H, Gly[2] α-CH); 3.742(dd, 1H, Gly[9] α-CH); 3.737(m, 2H, Gly[5] α-CH); 3.618 (dd, 1H, Gly[9] α-CH) 3.57 (dd, 1H, Gly[2] α-CH); 3.43 (m, 2H, Lol[11] β-CH_2); 3.388 (m, 1H, Phe$(NO_2)^3$ β-CH); 3.188 (m, 1H, Phe$(NO_2)^3$ β-CH); 2.239 (m, 2H, *n*Oct[0] β-CH_2); 1.926 (m, 1H, Ile[10] β-CH); 1.647 (m, 1H, Lol[11] β-CH); 1.636 (m, 2H, Leu[7] β-CH_2); 1.619 (m, 1H, Leu[7] γ-CH); 1.597 (m, 1H, Ile[10] γ-CH); 1.461 (s, 6H, Aib[4] β-CH_3); 1.574 (m, 2H, *n*Oct[0] γ-CH_2) 1.451 (s, 6H, Aib[8] β-CH_3) 1.428 (m, 1H, Lol[11] β-CH); 1.418 (s, 6H, Aib[1] β-CH_3); 1.283 (m, 8H, *n*Oct[0]); 1.276 (m, 1H, Ile[10] γ-CH); 1.198 (m, 1H, Lol[11] γ-CH); 0.925 (m, 3H, Ile[10] γ-CH3); 0.867 (m, 6H, Leu[7] δ-CH_3); 0.867 (m, 6H, Lol11 δ-CH3); 0.861 (m, 3H, *n*Oct[0] ω-CH_3); 0.841 (d, 3H, Ile[10] δ-CH_3).

Trichogin GA IV [Phe(NO_2)]^7 analog

^{1}H NMR (400 MHz, CD_3CN): 8.114 (m, 2H, Phe$(NO_2)^7$ arom.); 7.867 (t, 1H, Gly[6] NH); 7.727 (t, 1H, Gly[5] NH); 7.701 (d, 1H, Phe$(NO_2)^7$ NH); 7.653 (d, 1H, Leu[3] NH); 7.636 (t, 1H Gly[9] NH); 7.586 (s, 1H, Aib[8] NH); 7.516 (m, 2H, Phe$(NO_2)^7$ arom.); 7.479 (s, 1H, Aib[4] NH); 7.399 (t, 1H, Gly[2] NH); 7.269 (d, 1H, Ile[10] NH); 7.162 (s, 1H, Aib[1] NH); 6.609 (d, 1H, Lol[11] NH); 4.411 (m, 1H, Phe(NO2)[7] α-CH); 4.164 (m, 1H, Leu[3] α-CH); 4.015 (m, 1H, Ile[10] α-CH); 3.896 (m, 1H, Lol[11] α-CH); 3.784 (dd, 1H, Gly[2] α-CH); 3.757 (m, 2H, Gly[5] α-CH); 3.746 (m, 2H, Gly[6] α-CH); 3.668 (m, 2H, Gly[9] α-CH); 3.623 (dd, 1H, Gly[2] α-CH); 3.390 (m, 2H, Lol[11] β-CH_2); 3.389 (m, 1H, Phe$(NO_2)^7$ β-CH); 3.184 (m, 1H, Phe $(NO_2)^7$ β-CH); 2.211 (m, 2H, *n*Oct[0] β-CH_2); 1.917 (m, 1H, Ile[10] β-CH); 1.685 (m, 2H, Leu[3] β-CH_2); 1.660 (m, 1H, Leu[3] γ-CH) 1.585 (m, 2H, *n*Oct[0] γ-CH_2); 1.563 (m, 1H, Lol[11] β-CH_2); 1.557 (m, 1H, Ile[10] γ-CH); 1.474 (s, 6H, Aib[4] β-CH_3); 1.452 (s, 6H, Aib[8] β-CH_3); 1.392 (s, 6H, Aib[1] β-CH_3); 1.304 (m, 1H, Lol[11] γ-CH); 1.299 (m, 8H, *n*Oct[0] CH); 1.267 (m, 1H, Ile[10] γ-CH); 1.183 (m, 1H, Lol[11] γ-CH); 1.054 (m, 3H, Ile[10] δ-CH_3); 0.912 (m, 1H, Ile[10] γ-CH); 0.918 (m, 6H, Leu[3] δ-CH_3); 0.912 (m, 3H, Ile[10], γ-CH_3); 0.881 (m, 3H, *n*Oct[0] ω-CH_3); 0.822 (m, 6H, Lol[11] δ-CH_3).

Trichogin GA IV [Phe(NO_2)]^{10} analog

^{1}H NMR (400 MHz, CD_3CN): 8.114 (m, 2H, Phe$(NO_2)^{10}$ arom.); 7.928 (t, 1H, Gly[6] NH); 7.771 (t, 1H, Gly[5] NH); 7.694 (d, 1H Phe$(NO_2)^{10}$ NH); 7.685 (d, 1H, Leu[3] NH); 7.673 (t, 1H, Gly[9] NH); 7.615 (m, 2H, Phe$(NO_2)^{10}$ arom.); 7.598 (d, 1H, Leu[7] NH); 7.499 (s, 1H, Aib[4] NH); 7.456 (t, 1H, Gly[2] NH); 7.193 (s, 1H, Aib[1] NH); 6.953 (d, 1H, Lol[11] NH); 4.396 (m, 1H, Phe$(NO_2)^{10}$ α-CH); 4.222 (m, 1H, Leu[7] α-CH); 4.197 (m, 1H, Leu[3] α-CH); 3.957 (m, 1H, Lol[11] α-CH); 3.814 (m, 2H, Gly[6] α-CH); 3.788 (dd, 1H, Gly[2] α-CH); 3.747 (m, 2H, Gly[5] α-CH); 3.695 (dd, 1H, Gly[9] α-CH); 3.653 (dd, 1H Gly[2] α-CH); 3.508 (dd, 1H, Gly[9] α-CH); 3.456 (m, 2H, Lol[11] β-CH_2); 3.362 (dd, 1H, Phe$(NO_2)^{10}$ β-CH); 3.169 (dd, 1H, Phe$(NO_2)^{10}$ β-CH); 2.230 (t, 2H, *n*Oct[0] β-CH_2); 1.73 (m, 2H, Leu[7] β-CH_2); 1.698 (m, 2H, Leu[3] β-CH_2); 1.694 (m, 1H, Leu[7] γ-CH); 1.687 (m, 1H, Leu[3] γ-CH); 1.653 (m, 1H Lol[11] γ-CH); 1.594 (m, 2H, *n*Oct[0] γ-CH_2); 1.483 (s, 6H, Aib[4] β-CH_3); 1.456 (m, 1H, Lol[11] β-CH); 1.403 (s 6H, Aib[1] β-CH_3); 1.307 (m, 8H, *n*Oct[0]); 1.292 (m, 1H, Lol[11] γ-CH); 0.925 (m, 6H, Leu[3] δ-CH_3); 0.910 (m, 6H, Leu[7] δ-CH_3); 0.904 (m, 3H, *n*Oct[0] ω-CH_3); 0.894 (m, 6H, Lol[11] δ-CH_3).

FT-IR Absorption Spectroscopy

The FT-IR absorption spectra were recorded at 293 K using a Perkin-Elmer (Waltham, MA) model 1720X FT-IR spectrophotometer, nitrogen flushed, equipped with a sample-shuttle device, at 2 cm^{-1} nominal resolution, averaging 100 scans. Solvent (baseline) spectra were obtained under the same conditions. For spectral elaboration, the software SPECTRACALC provided by Galactic (Salem, MA) was employed. Cells with path lengths of 1.0 and 10 mm (with CaF_2 windows) were used. Spectrograde $CDCl_3$ (99.8%, *d*), CD_3CN (99.8%, d_3) and methanol were purchased from Merck (Darmstadt, Germany).

The attenuated total reflectance (ATR) measurements were obtained with a Nicolet-Nexus (Waltham, MA) instrument. A germanium crystal and a mercury cadmium telluride detector cooled to the liquid N_2 temperature were used. Averaged 100 scans between 4000 and 1000 cm^{-1} were performed.

Circular Dichroism Spectroscopy

The CD spectra were measured on a Jasco (Tokyo, Japan) model J-715 spectropolarimeter equipped with a Haake thermostat (Thermo Fisher Scientific, Waltham, MA). Baselines were corrected by subtracting the solvent contribution. A fused quartz cell of 1.0 mm path length (Hellma, Mühlheim, Germany) was used. The values are expressed in terms of $[\theta]_T$, the total molar ellipticity (deg × cm^2 × $dmol^{-1}$). Spectrograde 2,2,2-trifluoroethanol (TFE) (Acros Organics, Geel, Belgium) was employed as solvent. The CD measurements in TFE and in 100 mM aqueous sodium dodecyl sulfate (SDS) were carried out with a fused quartz cell of 0.5 mm path length.

Nuclear Magnetic Resonance Spectroscopy

A solution of [Phe(NO_2)][10]-trichogin GA IV (peptide concentration: 3.3 mM; pH 5) in a 100 mM SDS-d_{25} (CIL, Andover, MA) aqueous solution (9:1 H_2O/D_2O) was used for the 2D-NMR analysis. All NMR experiments were acquired on a Bruker Avance DMX-600 spectrometer using the TOPSPIN 1.3 software package, and recorded at 313 K. Suppression of the H_2O solvent signal was obtained by applying a WATERGATE gradient program. The spin systems of the trisubstituted amino acid residues were assigned with the use of the standard Wüthrich procedure [53]. DQF-COSY [54], CLEAN-TOCSY (spin-lock pulse, 70 ms) [55], and NOESY spectra were acquired by collecting 512 experiments, each one consisting of 32, 64, and 80 scans, respectively, and 2 K data points. To achieve the stereospecific assignment of the two diastereotopic methyl groups of the Aib residues, a C^β-selective heteronuclear multiple quantum coherence (HMQC) [56,57] experiment was acquired using selective excitation by means of Gaussian-shaped pulses with 1% truncation [58,59]. This C^β-selective HMQC experiment was recorded with 128 t_1 increments of 200 scans each and 2 K points. A spectral width of 16 ppm, centered at 22 ppm in F1, was employed. The sequential assignment was performed by means of the NOESY experiment (mixing time, 150 ms). A set of interproton distances was obtained by integration of the NOESY spectrum, using the SPARKY 3.111 software package, and was calibrated on the average of the values found for the interactions between the geminal protons of Gly and Leu residues, set to 1.78 Å. From the molecular dynamics (MD) calculations, carried out using the random simulated annealing (rSA) protocol of the XPLOR-NIH 2.9.6 program [60], 150 structures were generated. The topology of the nonstandard residue Phe(NO_2) was built from the parameters reported in the literature for nitrobenzene [61]. For distances involving equivalent or nonstereoassigned protons, an r^{-6} averaging was used. The MD calculations involved a minimization stage of 100 cycles, followed by SA and refinement stages. The SA consisted of 30 ps of dynamics at 1500 K (10 000 cycles in 3 fs steps) and 30 ps of cooling from 1500 to 100 K in 50 K decrements (15 000 cycles in 2 fs steps). The SA procedure, in which the

weights of NOE and nonbonded terms were gradually increased, was followed by 200 cycles of energy minimization. In the SA refinement stage, the system was cooled from 1000 to 100 K in 50 K decrements (20 000 cycles in 1 fs step). Finally, the calculations were completed with 200 cycles of energy minimization using a NOE force constant of 50 kcal/mol. The structures generated were visualized using the MOLMOL [62] version 2 K.2) program.

Liposome Leakage Assay

Peptide-induced leakage from small unilamellar vesicles (SUV) was measured at 293 K using the carboxyfluorescein (CF)-entrapped vesicle technique [63] and a Perkin–Elmer model MPF-66 spectrofluorimeter. CF-encapsulated SUV of egg phosphatidylcholine (PC)/cholesterol (Ch), 7:3, and phosphatidylethanolamine (PE)/phosphatidylglycerol (PG) were prepared by sonication in Hepes buffer, pH 7.4. The phospholipid concentration was kept constant (0.06 mM), and increasing peptide/lipid molar ratios (R^{-1}) were obtained by adding dimethylsulfoxide aliquots solutions of peptides, keeping the final concentration below 5% by volume. After rapid and vigorous stirring, the time course of fluorescence change corresponding to the CF escape was recorded at 520 nm (6 nm band pass) with λ_{exc} 488 nm (3 nm band pass). The percentage of released CF at time t was determined as $(F_t - F_0)/(F_T - F_0) \times 100$, with F_0 = fluorescence intensity of vesicles in the absence of peptide, F_t = fluorescence intensity at time t in the presence of peptide, and F_T = total fluorescence intensity determined by disrupting the vesicles by addition of 50 ml of a 10% Triton X-100 solution. The kinetics experiments were stopped at 20 min.

Antibacterial Activity Assays

Peptide antibacterial activity was tested against Gram-positive and Gram-negative bacteria by the standardized disk diffusion Bauer *et al.* method [64] using the Müller–Hinton culture medium, pH 7.2–7.4, recommended by the National Committee for Clinical Laboratory Standards [65] and 6-mm diameter disks. In the case of streptococci, a sheep-blood agar medium was exploited. Disks were prepared by using blank paper disks (Whatman, Maidstone, UK) previously autoclaved and saturated with the peptide solution. The peptide samples were dissolved in dimethylsulfoxide such as to give a 10 mg/ml solution. An inoculum size of 105 CFU (colony forming units)/ml (109 CFU/ml in case of *Pseudomonas aeruginosa*) was swabbed onto the test medium and left to dry at room temperature for about 15 min. The peptide-impregnated disks (100 mg/disk) were placed aseptically onto inoculated plates and incubated at 37 °C. The results were read after 24 h of incubation by measuring the inhibition zones (in millimeters). The antibacterial activity of peptides was tested against clinical isolates of bacteria and reference bacterial strains: *Staphylococcus aureus* ATCC 25923, *Streptococcus pyogenes* ATCC 19615, and *Escherichia coli* ATCC 25922, where ATCC stands for American Type Culture Collection strains. The well-known antibiotic tetracycline (10 μg/disk) was used as control test (Table 2).

Results and Discussion

Solid-Phase Peptide Synthesis

We prepared a set of three novel trichogin GA IV analogs, the primary structures of which are given in Table 1, where the Leu[3], Leu[7], and Ile[10] residues, respectively, are replaced by Phe(NO_2).

For the automatic SPPS of these three spectroscopically mono-labeled peptides, we applied our protocol for the preparation of trichogin GA IV (illustrated in Figure 2) [22,24,25,66] that is markedly improved with respect to that of Hjørringgard *et al* [67]. In Ref. [67], the authors reported isolated yields for the final trichogin GA IV of 20–24%, which should be compared

Table 2. Antibacterial activities of trichogin GA IV and its Phe(NO_2) analogs studied

Bacterial strain	Trichogin GA IV	3	7	10	Tetracycline[a]
Staphylococcus aureus ATCC 25923	15	7	8	12	31
Streptococcus pyogenes ATCC 19615	10	7	9	9	32
Escherichia coli ATCC 25922	0	0	0	0	28

[a]Control.

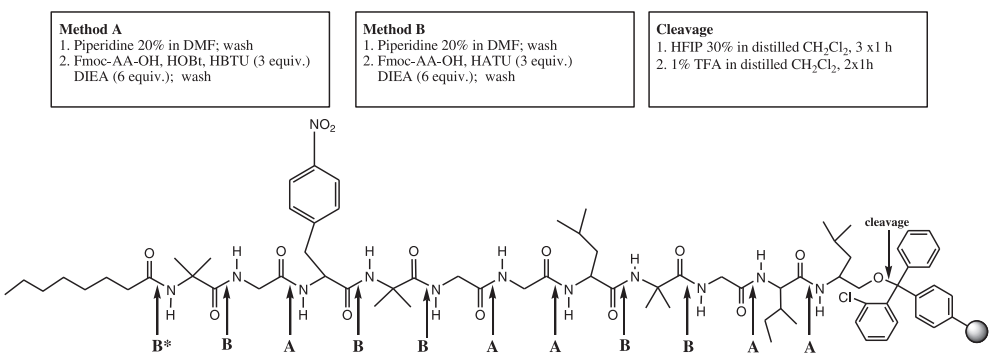

Figure 2. SPPS protocol for the preparation of the three Phe(NO_2) trichogin GA IV analogs (exemplified for the [Phe(NO_2)][3] analog). The B* coupling of the *n*Oct group was performed with *n*Oct-OH using the EDC/HOAt (2.5 equiv) C-activating method.

with the 79–83% yields obtained in the syntheses of our Phe (NO_2) trichogin GA IV analogs. We believe that the major factor responsible for these highly diverging yields has to be found in the different methods used to couple the next amino acid on the α-NH_2 functionality of the Aib residue (this side of Aib is well known to be dramatically critical for peptide bond formation [52]). Indeed, it is widely accepted that the HATU C-activation procedure (employed by us in this work) is by far more effective than the HBTU/HOBt procedure [49,50] used by Hjørringgard *et al.* [67].

Cleavage of peptides from the resin was (partially) achieved by treatment with 30% 1,1,1,3,3,3-hexafluoroisopropanol in distilled CH_2Cl_2 [48]. Although repeated three times, the yields of peptide recovery were rather modest (60–65%). A markedly improved outcome in removing the peptides from the resin was achieved by a subsequent treatment with a 1% TFA solution in distilled CH_2Cl_2. However, the HPLC profile of each crude synthetic material, in addition to the desired peptide alcohol, revealed the presence of a byproduct (Figure 3A), which was identified as the Lol trifluoroacetyl ester by MS (Figure 3B). The Lol primary alcoholic function was then fully regenerated by treatment of the peptide trifluoroacetate with 1 M HCl (gas) in diethyl ether in the presence of methanol for 60 min (transesterification).

Conformational Studies

The FT-IR absorption spectra of trichogin GA IV and its three Phe (NO_2) analogs in the amide A (3500–3200 cm^{-1}) region in $CDCl_3$ solution at 1 mM concentration (not shown) are dominated by a very intense band at 3313–3319 cm^{-1} (N–H stretching mode of H-bonded peptide groups [68–71]) accompanied by a very weak absorption between 3400 and 3450 cm^{-1} (N–H stretching mode of free peptide groups). These latter bands disappear upon increasing peptide concentration to 10 mM. This finding supports the view that a modest self-aggregation of the analogs does take place at concentration higher than 1 mM in this solvent of low polarity. In any case, even at the lowest concentration examined (0.1 mM), the main band at about 3315 cm^{-1} is still very intense, strongly suggesting that the conformation adopted by these three peptides is stabilized by an extensive set of intramolecular C=O. . .H–N H-bonds. The position of the strong amide I (C=O stretching mode) and amide II absorption maxima (1656–1658 cm^{-1} and 1540–1542 cm^{-1}, respectively) confirm that the conformation adopted is (3_{10}- and/or α-)helical [68–71]. The Leu (or Ile) to Phe (NO_2) replacements do not affect the FT-IR absorption spectrum of trichogin GA IV.

Because trichogin GA IV is known to interact with lipid membranes [15–40], our far-UV CD analysis on the three Phe (NO_2) trichogin GA IV analogs included two membrane mimetic environments, namely TFE and SDS micelles. The occurrence in each spectrum of two negative maxima near 205 and 222 nm (related to the parallel component of the $\pi \rightarrow \pi^*$ transition and the $n \rightarrow \pi^*$ transition of the peptide chromophore, respectively [72,73]) and one positive maximum at about 195 nm (related to the perpendicular component of the $\pi \rightarrow \pi^*$ transition) (Figure 4) suggests the presence of a well developed right-handed helical conformation.

The ellipticity ratio $R = [\theta]_{222}/[\theta]_{205}$ in the CD spectra affords a preliminary estimate of the prevailing helical type (whether 3_{10}- or α-) adopted by the three analogs investigated. This parameter is known to be lower than 0.35 for a large amount of 3_{10}-helix and higher than 0.70 for a high population of α-helix [74,75]. The experimentally observed R values are 0.77, 0.68, and 1.22 for the three Phe(NO_2) analogs at position 3, 7, or 10, respectively, in aqueous SDS (Figure 4B), whereas they are 0.46, 0.56, and 0.72 for the same analogs in TFE solution (Figure 4A). From these data, we can safely conclude that a high amount of α-helix occurs for all three analogs in aqueous SDS, while a mixed 3_{10}-/α-helix (with a largely prevailing α-helix component for the $[Phe(NO_2)]^{10}$ analog) is adopted in TFE. These observations are in general agreement with the known tendency of natural trichogin GA IV to fold into a well developed α-helix in aqueous SDS [16]. Interestingly, in both environments examined, the $[Phe(NO_2)]^{10}$ analog is remarkably more α-helical than its two isomeric peptides. A Phe(NO_2) model compound was reported to show very low ellipticities in the far-UV region [76,77]. As a result, nitroaromatic contributions are not expected to complicate the CD spectra in the region of the peptide Cotton effects for the Phe(NO_2) trichogin GA IV analogs investigated in this work.

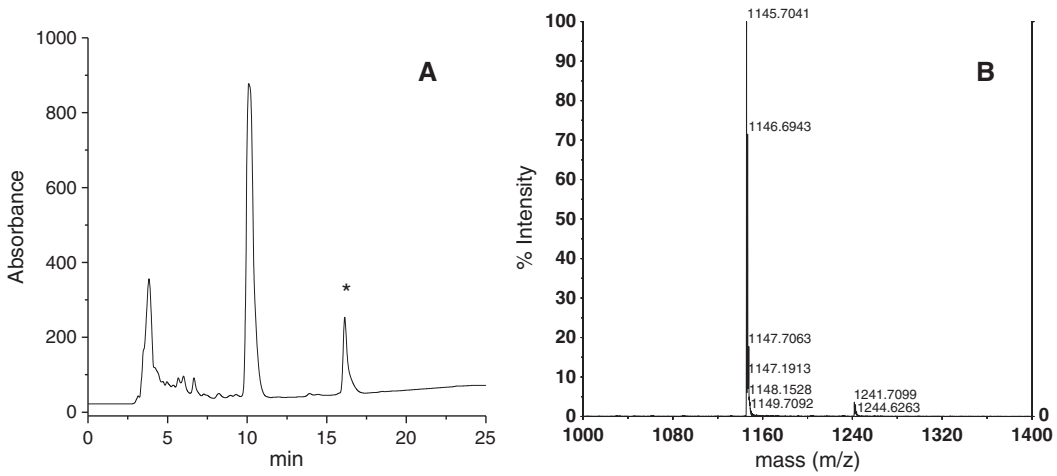

Figure 3. (A) HPLC profile and (B) mass spectrum of the crude synthetic $[Phe(NO_2)]^{10}$ trichogin GA IV analog. In part (A), the starred peak refers to the peptide ester byproduct. In part (B), the calculated mass difference between the peptide alcohol and its trifluoroacetyl ester (95.98 a.m.u.) is matched by the experimentally observed peaks (96.01 a.m.u.).

Journal of PeptideScience

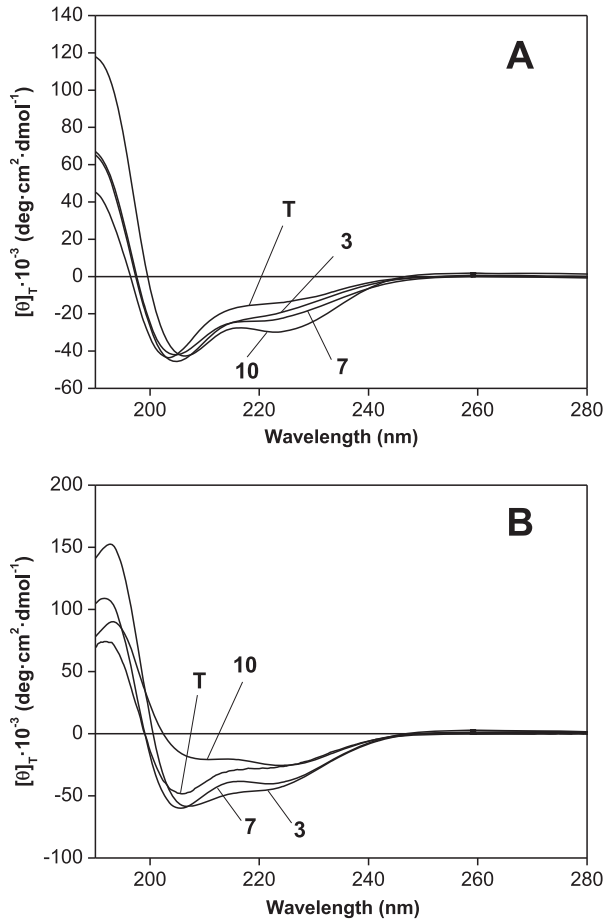

Figure 4. Far-UV CD spectra of the three Phe(NO_2) trichogin GA IV analogs in TFE (A) and 100 mM SDS aqueous solution (B).

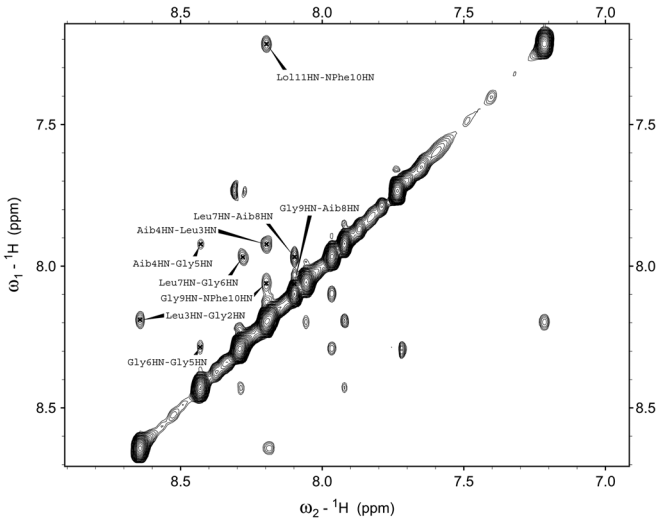

Figure 5. Amide proton region of the NOESY spectrum of the [Phe(NO_2)]^{10} trichogin GA IV analog [3.3 mM in 100 mM SDS-d_{25} aqueous solution (9:1 H_2O/D_2O), pH 5 (313 K, 600 MHz)].

Table 3. NOE constraints, deviations from idealized geometry, and mean energies for the NMR-based structures (energy <40 kcal/mol) of the [Phe(NO_2)]^{10} trichogin GA IV analog [3.3 mM in 100 mM SDS-d_{25} aqueous solution (9:1 H_2O/D_2O), pH 5 (313 K, 600 MHz)]

	Number of NOEs
Total	68
Intraresidue	25
Sequential	24
$i, i+n, n = 2, 3, 4$	19
Mean RMSD[a] from ideality of accepted structures	
Bonds (Å)	0.0029
Angles (°)	0.66
NOEs (Å)	0.067
Mean energies (kcal/mol) of accepted structures	
$E_{overall}$	36.47
E_{bond}	1.47
E_{angle}	18.75
E_{NOE}	14.47

[a]Root-mean-square deviation.

The 2D-NMR study of the representative [Phe(NO_2)]^{10} trichogin GA IV analog was conducted in a 100 mM SDS aqueous solution. This membrane-mimetic environment was chosen to compare the results with those obtained from the CD analysis described ealier. The proton resonances were fully assigned following the Wüthrich procedure [53]. The analysis of the heterocorrelated C^β-selective HMQC spectrum allowed us to complete the assignments of the resonances of the Aib residues, including the stereospecific assignment of the two prochiral methyl groups. In the NOESY spectrum, all of the nonoverlapping $NH_i \rightarrow NH_{i+1}$ sequential cross peaks, typical of a helical structure, are detected (Figure 5). Moreover, in the fingerprint region (not shown) several $C^\alpha H_i \rightarrow NH_{i+2}$, $C^\alpha H_i \rightarrow NH_{i+3}$, and $C^\alpha H_i \rightarrow NH_{i+4}$ cross peaks are seen, which account for a mixed 3_{10}-/α-helical conformation, such as those already reported for natural trichogin GA IV and some of its analogs [16,21,22,26]. However, the spectrum is characterized by a number of weak signals, probably because of the concomitant presence of a minor, perhaps less preferred, peptide conformation. These minor signals, overlapping with those belonging to the main conformation, make the NMR analysis more complicated, leading to a reduced number of unequivocal interproton correlations suitable to be employed in the restrained MD calculations. Yet, a total of 68 interproton distance restraints (Table 3) were derived and used in the rSA protocol to generate 150 3D structures, 110 of which had (i) violations to the NOE restraints lower than 0.5 Å; (ii) bond length deviation of <0.01 Å from the ideal geometry; and (iii) bond angle deviation of <1° from the ideal geometry. The 43 structures with a total energy of <40 kcal/mol were selected [backbone average RMSD, 0.84 (±0.27) Å]. The analysis of their averaged torsion angles (Table 4) reasonably suggests the coexistence of the α-helical and the 3_{10}-helical conformations, which nicely confirms the conclusions gained from the preliminary analysis of the NOESY spectrum. Interestingly, the conformationally diagnostic NOE cross peaks used in the MD calculations reported in Figure 6 seem to indicate a nonhomogeneous distribution of the two different (α- and 3_{10}-)helical types along the sequence. Indeed, the N-terminal part tends to be mostly 3_{10}-helical, whereas the C-terminal part is predominantly folded in an α-helix.

Table 4. Average values (°) for the ϕ_m and ψ_m torsion angles and their relative standard deviations resulting from the NMR-based structures (energy <40 kcal/mol) of the [Phe(NO_2)]^{10} trichogin GA IV analog [3.3 mM in 100 mM SDS-d_{25} aqueous solution (9:1 H_2O/D_2O), pH 5 (313 K, 600 MHz)]

Residue	ϕ_m	$\Delta\phi$	ψ_m	$\Delta\psi$
Aib^1	−53	±60	−12	±100
Gly^2	−155	±58	−78	±29
Leu^3	−51	±6	−30	±1
Aib^4	−52	±6	−22	±4
Gly^5	−78	±14	−11	±18
Gly^6	−65	±16	−23	±4
Leu^7	−65	±4	−41	±3
Aib^8	−74	±2	−21	±7
Gly^9	−79	±9	−52	±9
Phe(NO_2)^{10}	−64	±6	−12	±6
Lol^{11}	−132	±5	—	—

According to the MD calculations, the conformation switch takes place at the level of the –Gly^5–Gly^6– dipeptide, already known to be fairly flexible [22,27,28]. The lowest energy (33.72 kcal/mol) 3D structure is shown in Figure 7. Together with the aforementioned conformational switch, also helix amphiphilicity, a common feature of Aib-based peptaibiotics [8,66,78] is clearly visible. The presence of the polar –NO_2 group, lying on the hydrophobic face of the helix, might affect the known ability of the natural peptide to interact with biological membranes by perturbing its tendency to aggregate. However, the ability of the Phe aromatic ring, almost perpendicular to the helical axis, to stack might balance the aforementioned effect of the nitro group.

Taken together, the results of our MD calculations are consistent with the presence of an amphiphilic, mixed 3_{10}-/α-helical structure, with a change in the helical type at the level of the flexible Gly^5–Gly^6 central dipeptide. The spatial position adopted by the Phe(NO_2) residue is such as to balance its possible effects on the peptide biological activity.

Membrane Permeability Properties

The membrane modifying properties of the three Phe(NO_2) trichogin GA IV analogs were tested in comparison with those of the natural lipopeptaibiotic by measuring the induced leakage of CF entrapped in PC/Ch and PE/PG SUVs [63] (Figure 8).

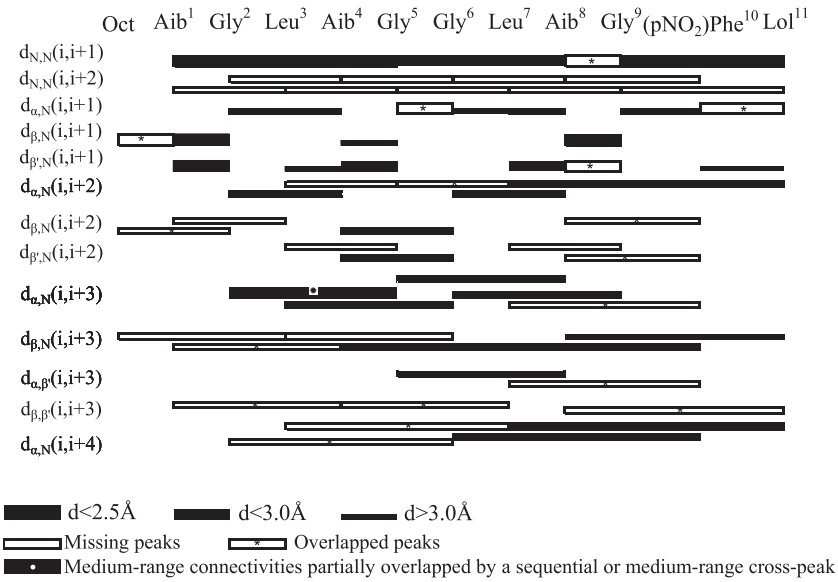

Figure 6. Summary of the significant interresidue NOESY cross peaks obtained for the [Phe(NO_2)]^{10} trichogin GA IV analog [3.3 mM in 100 mM SDS-d_{25} aqueous solution (9:1 H_2O/D_2O), pH 5 (313 K, 600 MHz)].

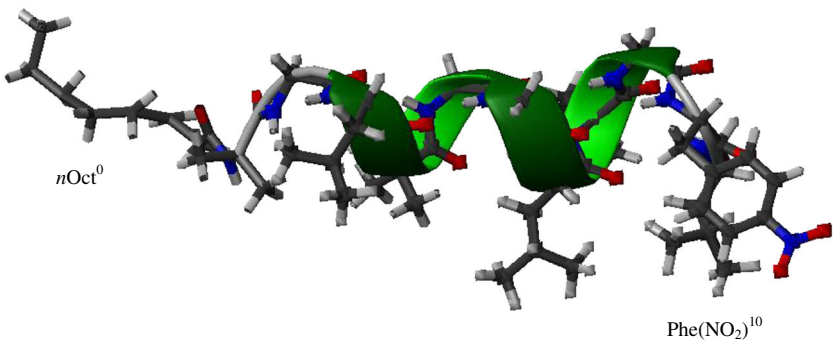

Figure 7. Ribbon representation of the lowest energy (33.7 kcal/mol) 3D structure obtained for the [Phe(NO_2)]^{10} trichogin GA IV analog [3.3 mM in 100 mM SDS-d_{25} aqueous solution (9:1 H_2O/D_2O), pH 5 (313 K, 600 MHz)].

Journal of PeptideScience

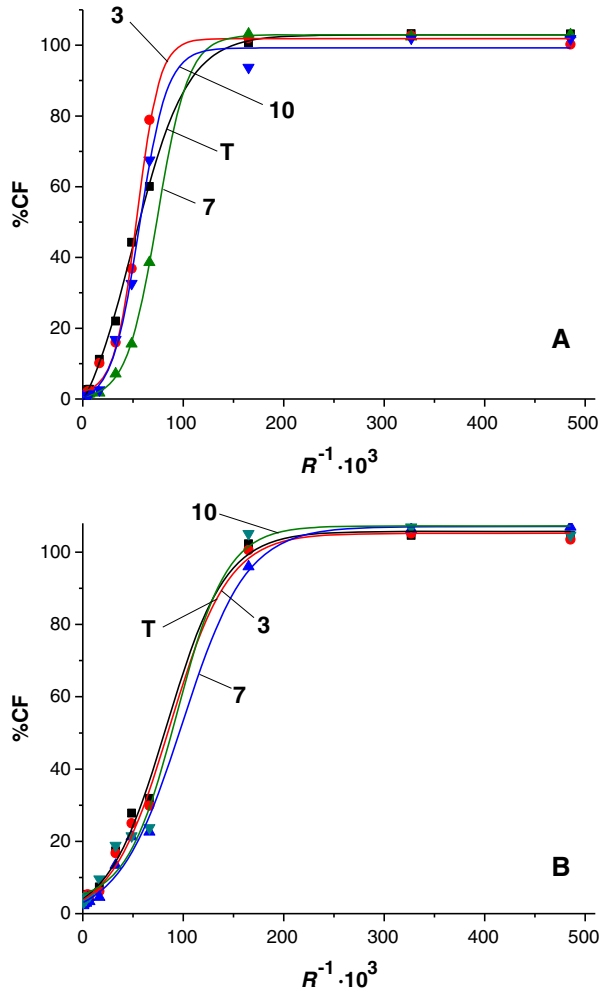

Figure 8. Peptide induced CF leakage at 20 min for different R^{-1} = [peptide]/[lipid] for PC/Ch (7:3) vesicles (A) and PE/PG (7:3) vesicles (B) for trichogin GA IV (T) and its three Phe(NO_2) analogs at position 3 (3),7 (7), or 10 (10).

The sigmoidal shape of the curves suggests that the permeability mechanism is largely cooperative. In other words, the peptides need to achieve a concentration high enough to form self-aggregates before the modifying process of the phospholipid bilayers could initiate. All three analogs are remarkably active in both membrane mimetic environments. More specifically, as compared with the activities of trichogin GA IV, in PC/Ch vesicles, the $[Phe(NO_2)]^3$ analog is the only one more active, although modestly, with the $[Phe(NO_2)]^{10}$ analog being equally effective. However, when the PE/PG vesicles are explored, the $[Phe(NO_2)]^3$ and $[Phe(NO_2)]^{10}$ analogs exhibit activities comparable with that of the reference parent compound. Interestingly, in both types of vesicles, the $[Phe(NO_2)]^7$ analog is less active, although not dramatically.

Antibacterial Activity

As reported in Table 2, in analogy with trichogin GA IV [10,15,22,24,25], we found that all three Phe(NO_2) analogs are active against two strains of *Gram*-positive bacteria, namely *S. aureus* and *S. pyogenes*, but inactive against the *Gram*-negative bacterium *E. coli*. The rank of activities against the *Gram*-positive bacteria decreases in the order $10 > 7 > 3$. However, their efficiencies against the *Gram*-positive bacteria are lower, albeit slightly, if compared with those of the natural lipopeptaibol. The well-known nonpeptide reference antibiotic tetracycline is markedly more active than trichogin GA IV and its analogs against all types of bacteria examined. Our present results confirm that trichogin GA IV is unable to penetrate the highly selective external membrane of the *Gram*-negative bacterial cells [10,22,24,25] and indicate that also its Phe(NO_2) analogs studied in this work share this property. Moreover, all four trichogin GA IV compounds are efficient against *Gram*-positive bacteria, which lack the external membrane but possess a thicker cellular wall.

Analysis of the Phe(NO_2) IR Absorption Probe

Recently, Brewer and coworkers [41] reported that Phe(NO_2), more specifically its nitroaromatic symmetric stretching mode near 1350 cm^{-1}, is a promising IR absorption probe of the polarity of local environments for peptide-based molecules. In the present work, we first examined the FT-IR absorption properties of our three Phe(NO_2) trichogin GA IV analogs single labeled at different positions in the peptide sequence with the aim at unraveling a potential shift of that band in response to modifications of the solvent polarity. To fully isolate the IR absorption of interest from all other bands exhibited by our peptide molecules, each of the spectra of the three Phe(F) (4-fluoro-phenylalanine) trichogin GA IV analogs, labeled at the same positions as those of the Phe(NO_2) peptide, recently prepared in our laboratory [79] and lacking the nitroaromatic chromophore, was subtracted from the corresponding spectrum of the Phe(NO_2) analog (the IR absorption maximum of the aromatic C–F group is known to occur in the 1250–1100 cm^{-1} region [80,81], well below that of the aromatic C–NO_2 group). As a representative example, the difference spectra for the $[Phe(NO_2)]^3$ analog in three solvents of different polarities ($CDCl_3$, MeOH, CD_3CN) are shown in Figure 9 (A, B, and C). The results were only partially encouraging in the sense that the position of the absorption maximum of the nitroaromatic chromophore moves slightly (from 1346 to 1348 cm^{-1}) as a function of the solvent properties. The same data were observed for the two other Phe(NO_2) analogs (spectra not shown).

Nevertheless, we decided to examine the behavior of the three Phe(NO_2) trichogin GA IV analogs in an environment that closely mimics that of lipid membranes where this lipopeptaibol is known to exert its bioactivity. To this end, we exploited ATR spectroscopy. The peptide samples, dissolved in a 4:1 CH_2Cl_2/MeOH solvent mixture, were incorporated in 5:1 PC/Ch liposomes. The mixture was deposited on the ATR crystal, and the solvent was evaporated under a N_2 stream. Figure 9D shows the ATR spectrum in the 1800–1300 cm^{-1} region of the $[Phe(NO_2)]^3$ analog with and without the contribution of the liposome. In both spectra, the Phe(NO_2) band stands out clearly at 1348 cm^{-1}. However, the corresponding absorptions for the $[Phe(NO_2)]^7$ and $[Phe(NO_2)]^{10}$ analogs (not shown) move to 1347 and 1345 cm^{-1}, respectively. It is clear that these modest spectral shifts provide only a limited information on the different polarities experienced by the Phe(NO_2) probe of the trichogin GA IV analogs in this membrane-mimetic environment.

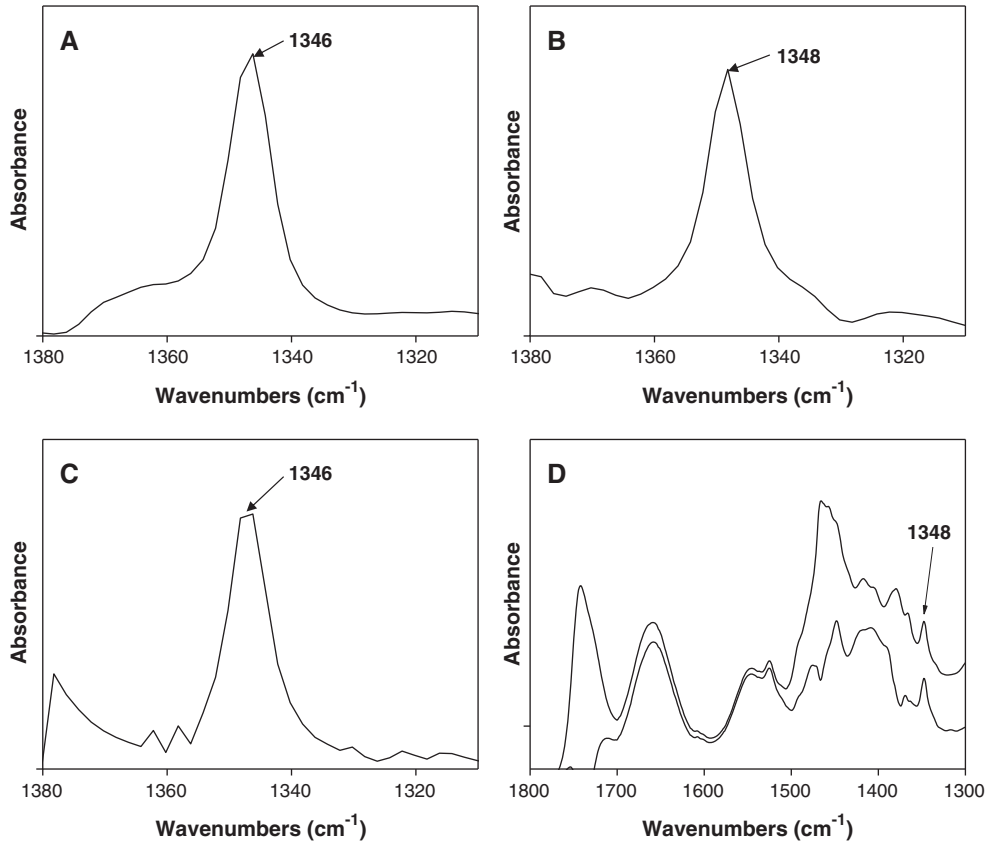

Figure 9. Different FT-IR absorption spectra in the 1380–1320 cm^{-1} region for the $[Phe(NO_2)]^3$ trichogin GA IV analog in $CDCl_3$ (A), CD_3CN (B), and MeOH (C) solutions. Part (D) shows the ATR spectra of the same peptide analog in the 1800–1300 cm^{-1} region with (top) and without (bottom) the contribution of the PC/Ch liposome.

Conclusions

In this paper, we reported the results of our investigation on three analogs of the 10-mer lipopeptaibol antibiotic trichogin GA IV, each of them mono-substituted with the IR absorption nitroaromatic label $Phe(NO_2)$. This mixed hydrophobic/hydrophilic probe was strategically introduced at position 3, 7, or 10 where it replaces a hydrophobic residue (Leu, Leu, or Ile, respectively). Our FT-IR absorption, CD, and 2D-NMR conformational findings support the view that, despite their slightly modified overall hydrophobicity and bulkiness, these analogs exhibit a solvent-dependent, mixed 3_{10}-/α-helical structure and a self-association tendency similar to those of the parent compound. Although partly attenuated, they also preserve its remarkable properties to disrupt model membranes and to exhibit good activity against *Gram*-positive bacteria.

Moreover, the main motivation of the present work, namely confirmation of the recently published, interesting application of the $Phe(NO_2)$ residue as a potential reporter group of ambient polarity in peptide-based molecules, was only partially successful because in all environments tested the observed range of the wavenumber of the absorption maximum of the symmetric $-NO_2$ stretching mode for the membrane-active trichogin GA IV analogs (1346–1348 cm^{-1}) is rather narrow. We tend to attribute this rather modest sensitivity to the absence of water in our environments (in contrast to the measurements performed in the original paper [41]). Indeed, effective hydrogen-bonding interactions between the hydrophilic nitro group and the solvent water molecules is a well-established phenomenon, which apparently is largely responsible for the published blue shift near 1350 cm^{-1}in the IR absorption spectrum of the $Phe(NO_2)$ label from tetrahydrofuran to aqueous solutions [41].

References

1 Toniolo C, Brückner H. *Peptaibiotics: Fungal Peptides Containing α-Dialkyl α-Amino Acids*. Verlag Helvetica Chimica Acta: Zürich, Switzerland and Wiley-VCH: Weinheim, Germany, 2009.
2 Karle IL, Balaram P. Structural characteristics of α-helical peptide molecules containing Aib residues. *Biochemistry* 1990; **29**: 6747–6756.
3 Toniolo C, Crisma M, Formaggio F, Peggion C. Control of peptide conformation by the Thorpe-Ingold effect (C^{α}-tetrasubstitution). *Biopolymers (Pept. Sci.)* 2001; **60**: 396–419.
4 Toniolo C, Crisma M, Bonora GM, Benedetti E, Di Blasio B, Pavone V, Pedone C, Santini A. Preferred conformation of the terminally blocked $(Aib)_{10}$ homo-oligopeptide. A long, regular 3_{10}-helix. *Biopolymers* 1991; **31**: 129–138.
5 Sansom MSP. The biophysics of peptide models of ion channels. *Prog. Biophys. Mol. Biol.* 1991; **55**: 139–235.
6 Crisma M, Peggion C, Baldini C, MacLean EJ, Vedovato N, Rispoli G, Toniolo C. Crystal structure of a spin-labeled, channel-forming alamethicin analogue. *Angew. Chem. Int. Ed.* 2007; **46**: 2047–2050.
7 Rebuffat S, Goulard C, Bodo B, Roquebert M-F. The peptaibol antibiotics from *Trichoderma* soil fungi: structural diversity and membrane properties. *Recent Res. Devel. Org. Biorg. Chem.* 1999; **3**: 65–91.
8 Toniolo C, Crisma M, Formaggio F, Peggion C, Epand RF, Epand RM. Lipopeptaibols, a novel family of membrane active antimicrobial peptides. *Cell. Mol. Life Sci.* 2001; **58**: 1179–1188.
9 Peggion C, Formaggio F, Crisma M, Epand RF, Epand RM, Toniolo C. Trichogin: a paradigm for lipopeptaibols. *J. Pept. Sci.* 2003; **9**: 679–689.
10 Auvin-Guette C, Rebuffat S, Prigent Y, Bodo B. Trichogin A IV, an 11-residue lipopeptaibol from *Trichoderma longibrachiatum*. *J. Am. Chem. Soc.* 1992; **114**: 2170–2174.

11 Toniolo C, Benedetti E. The polypeptide 3_{10}-helix. *Trends Biochem. Sci.* 1991; **16**: 350–353.
12 Benedetti E, Di Blasio B, Pavone V, Pedone C, Toniolo C, Crisma M. Characterization at atomic resolution of peptide helical structures. *Biopolymers* 1992; **32**: 453-456.
13 Bolin KA, Millhauser GL. α and 3_{10}: the split personality of polypeptide helices. *Acc. Chem. Res.* 1999; **32**: 1027–1033.
14 Toniolo C, Peggion C, Crisma M, Formaggio F, Shui X, Eggleston DS. Structure determination of racemic trichogin A IV using centrosymmetric crystals. *Nat. Struct. Biol.* 1994; **1**: 908–914.
15 Toniolo C, Crisma M, Formaggio F, Peggion C, Monaco V, Goulard C, Rebuffat S, Bodo B. Effect of N^{α}-acyl chain length on the membrane-modifying properties of synthetic analogs of the lipopeptaibol trichogin GA IV. *J. Am. Chem. Soc.* 1996; **118**: 4952–4958.
16 Monaco V, Locardi E, Formaggio F, Crisma M, Mammi S, Peggion E, Toniolo C, Rebuffat S, Bodo B. Solution conformational analysis of amphiphilic helical, synthetic analogs of the lipopeptaibol trichogin GA IV. *J. Pept. Res.* 1998; **52**: 261–272.
17 Formaggio F, Peggion C, Crisma M, Toniolo C. Short-chain analogues of the lipopeptaibol antibiotic trichogin GA IV: conformational analysis and membrane modifying properties. *J. Chem. Soc. Perkin Trans. 2* 2001; 1372–1377.
18 Gurunath R, Balaram P. A nonhelical, multiple β-turn conformation in a glycine-rich heptapeptide fragment of trichogin GA IV containing a single central α-aminoisobutyric acid residue. *Biopolymers* 1995; **35**: 21–29.
19 Monaco V, Formaggio F, Crisma M, Toniolo C, Shui X, Eggleston DS. Crystallographic structure of a multiple β-turn containing, glycine-rich heptapeptide: A synthetic precursor of the lipopeptaibol antibiotic trichodecenin I. *Biopolymers* 1996; **39**: 31–42.
20 Oancea S, Hilma G, Peggion C, Formaggio F, Toniolo C. Main-chain length control of conformation, membrane activity, and antibiotic properties of lipopeptaibol sequential analogues. *Chem. Biodivers.* 2008; **5**: 681–692.
21 De Zotti M, Biondi B, Peggion C, De Poli M, Fathi H, Oancea S, Toniolo C, Formaggio F. Partial thioamide scan on the lipopeptaibiotic trichogin GA IV. Effects on folding and bioactivity. *Beilstein J. Org. Chem.* 2012; **8**: 1161–1171.
22 De Zotti M, Biondi B, Park Y, Hahm K-S, Crisma M, Toniolo C, Formaggio F. Antimicrobial lipopeptaibol trichogin GA IV: role of the three Aib residues on conformation and bioactivity. *Amino Acids* 2012; **43**: 1761–1777.
23 Kropacheva TN, Raap J. Ion transport across a phospholipid membrane mediated by the peptide trichogin GA IV. *Biochim. Biophys. Acta* 2002; **1567**: 193–203.
24 De Zotti M, Biondi B, Formaggio F, Toniolo C, Stella L, Park Y, Hahm K-S. Trichogin GA IV: an antibacterial and protease-resistant peptide. *J. Pept. Sci.* 2009; **15**: 615–619.
25 De Zotti M, Biondi B, Peggion C, Formaggio F, Park Y, Hahm K-S, Toniolo C. Trichogin GA IV: a versatile template for the synthesis of novel peptaibiotics. *Org. Biomol. Chem.* 2012; **10**: 1285–1299.
26 Locardi E, Mammi S, Peggion E, Monaco V, Formaggio F, Crisma M, Toniolo C, Bodo B, Rebuffat S, Kamphuis J, Broxterman QB. Conformation and membrane activity of an analogue of the peptaibol antibiotic trichogin GA IV with a lipophilic amino acid at the N-terminus. *J. Pept. Sci.* 1998; **4**: 389–399.
27 Venanzi M, Bocchinfuso G, Gatto E, Palleschi A, Stella L, Formaggio F, Toniolo C. Metal binding properties of fluorescent analogues of trichogin GA IV: a conformational study by time-resolved spectroscopy and molecular mechanics investigations. *ChemBioChem* 2009; **10**: 91–97.
28 Venanzi M, Gatto E, Bocchinfuso G, Palleschi A, Stella L, Formaggio F, Toniolo C. Dynamics of formation of a helix-turn-helix structure in a membrane-active peptide: a time-resolved spectroscopic study. *ChemBioChem* 2006; **7**: 43–45.
29 Mazzuca C, Orioni B, Coletta M, Formaggio F, Toniolo C, Maulucci G, De Spirito M, Pispisa B, Venanzi M, Stella L. Fluctuations and the rate-limiting step of peptide-induced membrane leakage. *Biophys. J.* 2010; **99**: 1791–1800.
30 Bocchinfuso G, Palleschi A, Orioni B, Grande G, Formaggio F, Toniolo C, Park Y, Hahm K-S, Stella L. Different mechanisms of action of antimicrobial peptides: insight from fluorescence spectroscopy experiments and molecular dynamics simulations. *J. Pept. Sci.* 2009; **15**: 550–558.
31 Epand RF, Epand RM, Formaggio F, Crisma M, Wu H, Lehrer RI, Toniolo C. Analogs of the antimicrobial peptide trichogin having opposite membrane properties. *Eur. J. Biochem.* 2001; **268**: 703–712.
32 Mazzuca C, Stella L, Venanzi M, Formaggio F, Toniolo C, Pispisa B. Mechanism of membrane activity of the antibiotic trichogin GA IV: a two-state transition controlled by peptide concentration. *Biophys. J.* 2005; **88**: 3411–3421.
33 Venanzi M, Gatto E, Bocchinfuso G, Palleschi A, Stella L, Baldini C, Formaggio F, Toniolo C. Peptide folding dynamics: a time-resolved study from the nanosecond to the microsecond time regime. *J. Phys. Chem. B* 2006; **110**: 22834–22841.
34 Gatto E, Mazzuca C, Stella L, Venanzi M, Toniolo C, Pispisa B. Effect of peptide lipidation on membrane perturbing activity: a comparative study on two trichogin analogues. *J. Phys. Chem. B* 2006; **110**: 22813–22818.
35 Scrimin P, Veronese A, Tecilla P, Tonellato U, Monaco V, Formaggio F, Crisma M, Toniolo C. Metal ion modulation of membrane permeability induced by a polypeptide template. *J. Am. Chem. Soc.* 1996; **118**: 2505–2506.
36 Heuber C, Formaggio F, Baldini C, Toniolo C, Müller K. Multinuclear solid-state-NMR and FT-IR absorption investigations on lipid/trichogin bilayers. *Chem. Biodivers.* 2007; **4**: 1200–1218.
37 Milov AD, Erilov DA, Salnikov ES, Tsvetkov YD, Formaggio F, Toniolo C, Raap J. Structure and spatial distribution of the spin-labelled lipopeptide trichogin GA IV in a phospholipid membrane studied by pulsed electron–electron double resonance (PELDOR). *Phys. Chem. Chem. Phys.* 2005; **7**: 1794–1799.
38 Salnikov ES, Erilov DA, Milov AD, Tsvetkov YD, Peggion C, Formaggio F, Toniolo C, Raap J, Dzuba SA. Location and aggregation of the spin-labeled peptide trichogin GA IV in a phospholipid membrane as revealed by pulsed EPR. *Biophys. J.* 2006; **91**: 1532–1540.
39 Syryamina VN, Isaev NP, Peggion C, Formaggio F, Toniolo C, Raap J, Dzuba SA. Small-amplitude backbone motions of the spin-labeled lipopeptide trichogin GA IV in a lipid membrane as revealed by electron spin echo. *J. Phys. Chem. B* 2010; **114**: 12277–12283.
40 Syryamina VN, De Zotti M, Peggion C, Formaggio F, Toniolo C, Raap J, Dzuba SA. A molecular view on the role of cholesterol upon membrane insertion, aggregation, and water accessibility of the antibiotic lipopeptide trichogin GA IV as revealed by EPR. *J. Phys. Chem. B* 2012; **116**: 5653–5660.
41 Smith EE, Linderman BY, Luskin AC, Brewer SH. Probing local environments with the infrared probe: L-4-nitrophenylalanine. *J. Phys. Chem. B* 2011; **115**: 2380–2385.
42 Haiser K, Koller FO, Huber M, Regner N, Schrader TE, Schreier WJ, Zinth W. Nitro-phenylalanine: a novel sensor for heat transfer in peptides. *J. Phys. Chem. A* 2011; **115**: 2169–2175.
43 Murakami H, Hohsaka T, Ashizuka Y, Sisido M. Site-directed incorporation of *p*-nitrophenylalanine into streptavidin and site-to-site photoinduced electron transfer from a pyrenyl group to a nitrophenyl group on the protein framework. *J. Am. Chem. Soc.* 1998; **120**: 7520–7529.
44 Taki M, Hohsaka T, Murakami H, Taira K, Sisido M. Position-specific incorporation of a fluorophore – quencher pair into a single streptavidin through orthogonal four-base codon/anticodon pairs. *J. Am. Chem. Soc.* 2002; **124**: 14586–14590.
45 Tsao M-L, Summerer D, Ryu Y, Schultz PG. The genetic incorporation of a distance probe into proteins in *Escherichia coli*. *J. Am. Chem. Soc.* 2006; **128**: 4572–4573.
46 Barlos K, Chatzi O, Gatos D, Stavropoulos G. 2-Chlorotrityl chloride resin: studies on anchoring of Fmoc-amino acids and peptide cleavages. *Int. J. Pept. Protein Res.* 1991; **37**: 513–520.
47 Bollhagen R, Schmiedberger M, Barlos K, Grell E. A new reagent for the cleavage of fully protected peptides synthesized on 2-chlorotrityl chloride resin. *J. Chem. Soc., Chem. Commun.* 1994; 2559–2560.
48 Kocsis L, Ruff F, Orosz G. The effect of peptide length on the cleavage kinetics of 2-chlorotrityl resin-bound ethers. *J. Pept. Sci.* 2006; **12**: 428–436.
49 Carpino LA. 1-Hydroxy-7-azabenzotriazole. An efficient peptide coupling reagent. *J. Am. Chem. Soc.* 1993; **115**: 4397–4398.
50 Carpino LA, El-Faham A, Minor CA, Albericio F. Advantageous applications of azabenzotriazole (triazolopyridine)-based coupling reagents to solid-phase peptide synthesis. *J. Chem. Soc., Chem. Commun.* 1994; 201–203.
51 König W, Geiger R. Eine neue Methode zur Synthese von Peptiden: Aktivierung der Carboxylgruppe mit Dicyclohexylcarbodiimid unter Zusatz von 1-Hydroxy-benzotriazolen. *Chem. Ber.* 1970; **103**: 788–798.
52 Formaggio F, Broxterman QB, Toniolo C. In *Houben-Weyl: Methods of Organic Synthesis*, Vol. E22c, Goodman M, Felix A, Moroder L, Toniolo C (eds.). Thieme: Stuttgart, Germany, 2003; 292–310.

53 Wüthrich K. *NMR of Proteins and Nucleic Acids*. Wiley: New York, 1986.
54 Rance M, Sørensen OW, Bodenhausen G, Wagner G, Ernst RR, Wüthrich K. Improved spectral resolution in COSY ^{1}H NMR spectra of proteins via double quantum filtering. *Biochem. Biophys. Res. Commun.* 1983; **117**: 479–485.
55 Griesinger C, Otting G, Wüthrich K, Ernst RR. Clean TOCSY for proton spin system identification in macromolecules. *J. Am. Chem. Soc.* 1988; **110**: 7870–7872.
56 Bax A, Subramanian S. Sensitivity-enhanced two-dimensional heteronuclear shift correlation NMR spectroscopy. *J. Magn. Reson.* 1986; **67**: 565–569.
57 Bax A, Summers MF. Proton and carbon-13 assignments from sensitivity-enhanced detection of heteronuclear multiple-bond connectivity by 2D multiple quantum NMR. *J. Am. Chem. Soc.* 1986; **108**: 2093–2094.
58 Bauer C, Freeman R, Frenkiel T, Keeler J, Shaka AJ. Gaussian pulses. *J. Magn. Reson.* 1984; **58**: 442–457.
59 Emsley L, Bodenhausen G. Self-refocusing effect of 270° Gaussian pulses. Applications to selective two-dimensional exchange spectroscopy. *J. Magn. Reson.* 1989; **82**: 211–221.
60 Schwieters CD, Kuszewski JJ, Tjandra N, Clore MG. The X-PLOR-NIH NMR molecular structure determination package. *J. Magn. Reson.* 2003; **160**: 65–73.
61 Malde AK, Zuo L, Breeze M, Stroet M, Poger D, Nair PC, Oostenbrink C, Mark AE. An automated force field topology builder (ATB) and repository: version 1.0. *J. Chem. Theory Comput.* 2011; **7**: 4026–4037.
62 Koradi R, Billeter M, Wüthrich K. MOLMOL: A program for display and analysis of macromolecular structures. *J. Mol. Graph.* 1996; **14**: 51–55.
63 El Hajji M, Rebuffat S, Le Doan T, Klein G, Satre M, Bodo B. Interaction of trichorzianines A and B with model membranes and with the amoeba *Dictyostalium*. *Biochim. Biophys. Acta* 1989; **978**: 97–104.
64 Bauer AW, Kirby WM, Sherris JC, Turck M. Antibiotic susceptibility testing by a standardized single disk method. *Am. J. Clin. Pathol.* 1966; **45**: 493–496.
65 *National Committee for Clinical Laboratory Standards* M2-A6, Wayne, PA, 1997.
66 De Zotti M, Biondi B, Peggion C, Park Y, Hahm K-S, Formaggio F, Toniolo C. Synthesis, preferred conformation, protease stability, and membrane activity of heptaibin, a medium-length peptaibiotic. *J. Pept. Sci.* 2011; **17**: 585–594.
67 Hjørringgaard CU, Pedersen JM, Vosegaard T, Nielsen NC, Skrydstrup T. An automatic solid-phase synthesis of peptaibols. *J. Org. Chem.* 2009; **74**: 1329–1332.
68 Bellamy M. *The Infra-Red Spectra of Complex Molecules*. 2nd edn, Methuen: London, U.K., 1966.
69 Baron MH, De Lozé C, Toniolo C, Fasman GD. Structure in solution of protected homo-oligopeptides of L-valine, L-isoleucine, and L-phenylalanine: an infrared absorption study. *Biopolymers* 1978; **17**: 2225–2239.
70 Moretto V, Crisma M, Bonora GM, Toniolo C, Balaram H, Balaram P. Comparison of the effect of five guest residues on the β-sheet conformation of host (L-Val)$_n$ homo-oligopeptides. *Macromolecules* 1989; **22**: 2939–2944.
71 Kennedy DF, Crisma M, Toniolo C, Chapman D. Studies of peptides forming 3_{10}- and α-helices and β-bend ribbon structures in organic solution and in model biomembranes by Fourier transform infrared spectroscopy. *Biochemistry* 1991; **30**: 6541–6548.
72 Beychok S. Circular dichroism of poly-α-amino acids and proteins. In *Poly-α-Amino Acids: Protein Models for Conformational Studies*, Fasman GD (ed.). Dekker: New York, 1967; 293–337.
73 Manning MC, Woody RW. Theoretical CD studies of polypeptide helices: examination of important electronic and geometric factors. *Biopolymers* 1992; **31**: 569–586.
74 Toniolo C, Polese A, Formaggio F, Crisma M, Kamphuis J. Circular dichroism spectrum of a peptide 3_{10}-helix. *J. Am. Chem. Soc.* 1996; **118**: 2744–2745.
75 Formaggio F, Crisma M, Rossi P, Scrimin P, Kaptein B, Broxterman QB, Kamphuis J, Toniolo C. The first water-soluble 3_{10}-helical peptides. *Chem. Eur. J.* 2000; **6**: 4498–4504.
76 Goodman M, Toniolo C, Peggion E. Conformational aspects of polypeptides. XXIX. Conformational assignments for some aromatic polypeptides by far-UV Cotton effects. New results. *Biopolymers* 1968; **6**: 1691-1695.
77 Toniolo C, Falxa ML, Goodman M. Conformational aspects of polypeptides. XXV. Solvent and temperature effects on the conformations of copolymers of benzyl and methyl L-aspartate with nitrobenzyl L-aspartate. *Biopolymers* 1968; **6**: 1579–1603.
78 De Zotti M, Damato F, Formaggio F, Crisma M, Schievano E, Mammi S, Kaptein B, Broxterman QB, Felock PJ, Hazuda DJ, Singh SB, Kirschbaum J, Brückner H, Toniolo C. Total synthesis, characterization, and conformational analysis of the naturally occurring hexadecapeptide integramide A and its diastereomer at positions 14 and 15. *Chem. Eur. J.* 2010; **16**: 316–327.
79 Battistella C. *Chemistry Degree Thesis*. University of Padova: Italy, 2011.
80 Silverstein RM, Webster FX. *Spectrometric Identification of Organic Compounds*. Wiley: New York, 1998.
81 Jackson RFW, Moore RJ, Dexter CS, Elliott J, Mowbray CE. Concise synthesis of enantiomerically pure phenylalanine, homophenylalanine, and bishomophenylalanine derivatives using organozinc chemistry: NMR studies of amino acid-derived organozinc reagents. *J. Org. Chem.* 1998; **63**: 7875–7884.

